

Article

## Bifurcation and complex dynamics of a discrete-time predator–prey system involving group defense

S. M. Sohel Rana

Department of Mathematics, University of Dhaka, Dhaka-1000, Bangladesh

E-mail: srana.mthdu@gmail.com

Received 1 May 2015; Accepted 10 June 2015; Published 1 September 2015



### Abstract

In this paper, we investigate the dynamics of a discrete-time predator-prey system involving group defense. The existence and local stability of positive fixed point of the discrete dynamical system is analyzed algebraically. It is shown that the system undergoes a flip bifurcation and a Neimark-Sacker bifurcation in the interior of  $R_+^2$  by using bifurcation theory. Numerical simulation results not only show the consistence with the theoretical analysis but also display the new and interesting dynamical behaviors, including phase portraits, period-7, 20-orbits, attracting invariant circle, cascade of period-doubling bifurcation from period-20 leading to chaos, quasi-periodic orbits, and sudden disappearance of the chaotic dynamics and attracting chaotic set. The Lyapunov exponents are numerically computed to characterize the complexity of the dynamical behaviors.

**Keywords** discrete-time predator-prey system; chaos; flip and Neimark-Sacker bifurcations; Lyapunov exponents.

Computational Ecology and Software  
ISSN 2220-721X  
URL: <http://www.iaees.org/publications/journals/ces/online-version.asp>  
RSS: <http://www.iaees.org/publications/journals/ces/rss.xml>  
E-mail: [ces@iaees.org](mailto:ces@iaees.org)  
Editor-in-Chief: WenJun Zhang  
Publisher: International Academy of Ecology and Environmental Sciences

### 1 Introduction

It is well known the Lotka-Volterra predator-prey model is one of the fundamental population models; a predator-prey interaction has been described firstly by two pioneers Lotka (1924) and Volterra (1926) in two independent works. After them, more realistic prey-predator model were introduced by Holling suggesting three types of functional responses for different species to model the phenomena of predation (Holling, 1965). Qualitative analyses of prey-predator models describe by set of differential equations were studied by many authors (Brauer and Castillo, 2001; Hastings and Powell, 1991; Klebanoff and Hastings, 1994; Murray, 1998; Zhu et al., 2002). Another possible way to understand a prey-predator interaction is by using discrete-time models. In recent years, many authors (Brauer and Castillo, 2001; Murray, 1998; Agiza et al., 2009; Danca et al., 1997; Elsadany et al., 2012; Hasan et al., 2012; He and Lai, 2011; Jing and Yang, 2006; Li and Yorke, 1975; Liu and Xiao, 2007; Hu et al, 2011; He and Li, 2014) have suggested that discrete time models governed by difference equations are more appropriate than the continuous ones, especially when the populations have

non-overlapping generations. These models are more reasonable showing that the dynamics of the discrete-time prey-predator models can present a much richer set of patterns than those observed in continuous-time models and lead to unpredictable dynamic behaviors from a biological point of view. However, there are few articles discussing the dynamical behaviors of predator-prey models, which include bifurcations and chaos phenomena for the discrete-time models. The authors (He and Lai, 2011; Jing and Yang, 2006; Liu and Xiao, 2007; Hu et al, 2011) obtained the flip bifurcation and Hopf bifurcation by using the center manifold theorem and bifurcation theory, while in Agiza et al. (2009), Danca et al. (1997), Elsadany et al. (2012), the authors only showed the flip bifurcation and Hopf bifurcation by using numerical simulations. But in (Wang and Li, 2014; Ghaziani, 2014; Rana, 2015), the authors showed that the system undergoes a flip bifurcation and/or a Neimark-Sacker bifurcation by using bifurcation theory.

In this paper, we consider the following system of ordinary differential equations of generalized Gauss-type as a model (Freedman and Wolkowicz, 1986) of predator-prey interaction with group defense exhibited by the prey:

$$\begin{aligned}\dot{x} &= xg(x, K) - yp(x) \\ \dot{y} &= y(-d + q(x))\end{aligned}\tag{1}$$

where  $x$  and  $y$  are functions of time representing population densities of prey and predator, respectively;  $K > 0$  is the carrying capacity of the prey and  $d > 0$  is the death rate of the predator. The function  $g(x, K)$  represents the specific growth rate of the prey in the absence of predator. A prototype is the logistic

growth,  $g(x, K) = r\left(1 - \frac{x}{K}\right)$ , with intrinsic growth rate  $r$ . The function  $p(x)$  denotes the predator

response function and we assume it is of the Holling type II form,  $p(x) = \frac{mx}{\beta + x}$ . The rate of conversion of

prey to predator is described by  $q(x)$ . In Gause's model,  $q(x) = cp(x)$  for some positive constant  $c$ .

Without loss of generality, by scaling the parameters, we first write the system (1) in the specific form (Rosenzweig and MacArthur, 1963)

$$\begin{aligned}\dot{x} &= rx\left(1 - \frac{x}{K}\right) - \frac{xy}{\beta + x} \\ \dot{y} &= y\left(-d + \frac{\alpha x}{\beta + x}\right)\end{aligned}\tag{2}$$

where  $r, K, d, \alpha$  and  $\beta$  are positive parameters. Applying the forward Euler scheme to system (2), we obtain the discrete-time predator-prey system as follows:

$$H : \begin{pmatrix} x \\ y \end{pmatrix} \rightarrow \begin{pmatrix} x + \delta \left[ rx(1 - x/K) - \frac{xy}{\beta + x} \right] \\ y + \delta \left[ -dy + \frac{\alpha xy}{\beta + x} \right] \end{pmatrix} \quad (3)$$

where  $\delta$  is the step size. In this paper, we only restrict our attention to investigate this version as a discrete-time dynamical system in the closed first quadrant  $R_+^2$  by using bifurcation theory and center manifold theory (see section 4, Kuznetsov, 1998). We rigorously prove that this discrete model possesses the flip bifurcation and the Neimark-Sacker bifurcation. Meanwhile, numerical simulations are presented not only to illustrate our results with the theoretical analysis, but also to exhibit the complex dynamical behaviors such as the cascade periodic-doubling bifurcation in periods 7, 20-orbits, quasi-periodic orbits and chaotic sets. These results reveal far richer dynamics of the discrete model compared with the continuous model. In particular; we observe that when the prey is in chaotic dynamic, the predator can tend to extinction or to a stable equilibrium. The computations of Lyapunov exponents confirm the dynamical behaviors. The analysis and results in this paper are interesting in mathematics and biology.

This paper is organized as follows. In Section 2, we discuss the existence and local stability of positive fixed point for system (3) in  $R_+^2$ . In Section 3, we show that there exist some values of the parameters such that (3) undergoes the flip bifurcation and the Neimark-Sacker bifurcation in the interior of  $R_+^2$ . In section 4, we present the numerical simulations including the bifurcation diagrams, the phase portraits at neighborhood of critical values and the maximum Lyapunov exponents corresponding to the bifurcation diagrams. Finally a short discussion is given in Section 5.

## 2 Existence and Stability of Fixed Points

In this section, we first determine the existence of the fixed points of the system (3), then investigate their stability by the eigenvalues for the Jacobian matrix of (3) at the fixed point.

It is clear that the fixed points of (3) satisfy the following equations:

$$\begin{cases} x + \delta \left[ rx(1 - x/K) - \frac{xy}{\beta + x} \right] = x \\ y + \delta \left[ -dy + \frac{\alpha xy}{\beta + x} \right] = y \end{cases} \quad (4)$$

By a simple algebraic computation, it is straightforward to obtain the following results:

### Lemma 1.

- (i) For all parameter values, (3) has two fixed points,  $E_0(0,0)$  and  $E_1(K,0)$ ;
- (ii) if  $0 < \frac{\beta d}{\alpha - d} < K$ , then (3) has, additionally, a unique positive fixed point,  $E_2(x^*, y^*)$ , where

$$x^* = \frac{\beta d}{\alpha - d} \quad \text{and} \quad y^* = r(1 - x^*/K)(\beta + x^*).$$

Fig. 1 shows the distribution of the fixed points for  $K=1$  in the space  $(\alpha, \beta, d)$ . There is an unique

positive fixed point in the region (II), and no positive fixed point on the surface  $C$  and the region (I), where

$$\text{surface } C = \left\{ (\alpha, \beta, d) : \frac{\beta d}{\alpha - d} = K \right\}.$$

Now we investigate the stability of the fixed points for (3). The Jacobian matrix of the system (3) at a fixed point  $\bar{E}(\bar{x}, \bar{y})$  is

$$J(\bar{x}, \bar{y}) = \begin{pmatrix} 1 + \delta a_1 & -\delta b_1 \\ \delta a_2 & 1 + \delta b_2 \end{pmatrix} \tag{5}$$

where

$$\begin{aligned} a_1 &= r \left( 1 - \frac{2\bar{x}}{K} \right) - \frac{\beta \bar{y}}{(\beta + \bar{x})^2}, b_1 = \frac{\bar{x}}{\beta + \bar{x}} \\ a_2 &= \frac{\alpha \beta \bar{y}}{(\beta + \bar{x})^2}, b_2 = -d + \frac{\alpha \bar{x}}{\beta + \bar{x}} \end{aligned} \tag{6}$$

The characteristic equation associated with (5) is

$$\lambda^2 - \text{tr}J \lambda + \det J = 0 \tag{7}$$

where  $\lambda$  is the eigenvalue of (5) and

$$\begin{aligned} \text{tr}J &= 2 + \delta(a_1 + b_2) \\ \det J &= 1 + \delta(a_1 + b_2) + \delta^2(a_1 b_2 + a_2 b_1) \end{aligned} \tag{8}$$

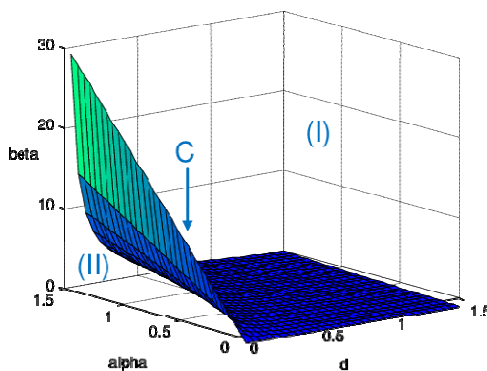


Fig. 1 Distribution of fixed point of map (3) for  $K = 1$ .

Hence the system (3) is

- (i) a dissipative dynamical system if and only if

$$\left| 1 + \delta(a_1 + b_2) + \delta^2(a_1 b_2 + a_2 b_1) \right| < 1;$$

- (ii) a conservative dynamical system if and only if

$$\left| 1 + \delta(a_1 + b_2) + \delta^2(a_1 b_2 + a_2 b_1) \right| = 1;$$

- (iii) an undissipated dynamical system otherwise.

In the following we deduce the local dynamics of the positive fixed point  $E_2(x^*, y^*)$  only (we left the others). Note that the local stability of the fixed point  $(x^*, y^*)$  is determined by the modules of eigenvalues of the characteristic equation at the fixed point.

The Jacobian matrix due to the linearization of (3) evaluated at  $E_2$  is given by

$$J(x^*, y^*) = \begin{pmatrix} 1 + \delta a_1 & -\delta b_1 \\ \delta a_2 & 1 + \delta b_2 \end{pmatrix} \quad (9)$$

and the corresponding characteristic equation of (9) can be written as

$$F(\lambda) = \lambda^2 - \text{tr}J \lambda + \det J = 0 \quad (10)$$

where  $a_1, b_1, a_2, b_2, \text{tr}J$  and  $\det J$  are determined by (6) and (8) with  $\bar{x}$  &  $\bar{y}$  are replaced by  $x^*$  &  $y^*$  respectively.

Therefore, the eigenvalues of (10) are

$$\lambda_{1,2} = \frac{\text{tr}J \pm \sqrt{(\text{tr}J)^2 - 4 \det J}}{2} \quad (11)$$

where  $(\text{tr}J)^2 - 4 \det J = \delta^2 \Delta$  and  $\Delta = (a_1 - b_2)^2 - 4a_2b_1$ .

Using Jury's criterion (Elaydi, 1996), we have necessary and sufficient condition for local stability of the fixed point  $E_2$  which are given in the following proposition.

**Proposition 1.** Let  $E_2$  be a positive fixed point of (3). Then

(i) it is a sink if one of the following conditions holds:

$$(i.1) \quad \Delta \geq 0 \text{ and } \delta < \frac{-(a_1 + b_2) - \sqrt{\Delta}}{a_1b_2 + a_2b_1};$$

$$(i.2) \quad \Delta < 0 \text{ and } \delta < -\frac{a_1 + b_2}{a_1b_2 + a_2b_1}.$$

(ii) it is a source if one of the following conditions holds:

$$(ii.1) \quad \Delta \geq 0 \text{ and } \delta > \frac{-(a_1 + b_2) + \sqrt{\Delta}}{a_1b_2 + a_2b_1};$$

$$(ii.2) \quad \Delta < 0 \text{ and } \delta > -\frac{a_1 + b_2}{a_1b_2 + a_2b_1}.$$

(iii) it is non-hyperbolic if one of the following conditions holds:

$$(iii.1) \quad \Delta \geq 0 \text{ and } \delta = \frac{-(a_1 + b_2) \pm \sqrt{\Delta}}{a_1 b_2 + a_2 b_1};$$

$$(iii.2) \quad \Delta < 0 \text{ and } \delta = -\frac{a_1 + b_2}{a_1 b_2 + a_2 b_1}.$$

(iv) it is a saddle for the other values of parameters except those values in (i)–(iii).

Following Jury’s criterion, we can see that one of the eigenvalues of  $J(E_2)$  is  $-1$  and the others are neither  $1$  nor  $-1$  if the term (iii.1) of Proposition 1 holds. Therefore, there may be flip bifurcation of the fixed point  $E_2$  if  $\delta$  varies in the small neighborhood of  $FB1_{E_2}$  or  $FB2_{E_2}$  where

$$FB1_{E_2} = \left\{ (r, K, d, \alpha, \beta, \delta) \in (0, +\infty) : \delta = \frac{-(a_1 + b_2) - \sqrt{\Delta}}{a_1 b_2 + a_2 b_1}, \Delta \geq 0, \alpha > d, \& \frac{\beta d}{\alpha - d} < K \right\}$$

or

$$FB2_{E_2} = \left\{ (r, K, d, \alpha, \beta, \delta) \in (0, +\infty) : \delta = \frac{-(a_1 + b_2) + \sqrt{\Delta}}{a_1 b_2 + a_2 b_1}, \Delta \geq 0, \alpha > d, \& \frac{\beta d}{\alpha - d} < K \right\}.$$

Also when the term (iii.2) of Proposition 1 holds, we can obtain that the eigenvalues of  $J(E_2)$  are a pair of conjugate complex numbers with module one. The conditions in the term (iii.2) of Proposition 1 can be written as the following set:

$$NS_{E_2} = \left\{ (r, K, d, \alpha, \beta, \delta) \in (0, +\infty) : \delta = -\frac{a_1 + b_2}{a_1 b_2 + a_2 b_1}, \Delta < 0, \alpha > d, \& \frac{\beta d}{\alpha - d} < K \right\},$$

and if the parameter  $\delta$  varies in the small neighborhood of  $NS_{E_2}$ ; then the Neimark-Sacker bifurcation will appear.

### 3 Flip Bifurcation and Neimark-Sacker Bifurcation

In this section, we choose the parameter  $\delta$  as a bifurcation parameter to study the flip bifurcation and the Neimark-Sacker bifurcation of  $E_2$  by using bifurcation theory in (see Section 4 in Kuznetsov, 1998; see also Guckenheimer and Holmes, 1983; Robinson, 1999; Wiggins, 2003).

We first discuss the flip bifurcation of (3) at  $E_2$ . Suppose that  $\Delta > 0$ , i.e.,

$$(a_1 - b_2)^2 - 4a_2 b_1 > 0 \tag{12}$$

$$\text{If } \delta = \delta_1 = \frac{-(a_1 + b_2) - \sqrt{\Delta}}{a_1 b_2 + a_2 b_1}$$

or

$$\delta = \delta_1 = \frac{-(a_1 + b_2) + \sqrt{\Delta}}{a_1 b_2 + a_2 b_1},$$

then the eigenvalues of  $J$  given by (11) are  $\lambda_1(\delta_1) = -1$  and  $\lambda_2(\delta_1) = 3 + \delta_1(a_1 + b_2)$ .

The condition  $|\lambda_2(\delta_1)| \neq 1$  leads to

$$\delta_1(a_1 + b_2) \neq -2, -4. \quad (13)$$

Let  $\tilde{x} = x - x^*$ ,  $\tilde{y} = y - y^*$  and  $A(\delta) = J(x^*, y^*)$ , we transform the fixed point  $(x^*, y^*)$  of system (3) into the origin, then system (3) becomes

$$\begin{pmatrix} \tilde{x} \\ \tilde{y} \end{pmatrix} \rightarrow A(\delta) \begin{pmatrix} \tilde{x} \\ \tilde{y} \end{pmatrix} + \begin{pmatrix} F_1(\tilde{x}, \tilde{y}, \delta) \\ F_2(\tilde{x}, \tilde{y}, \delta) \end{pmatrix} \quad (14)$$

where

$$\begin{aligned} F_1(\tilde{x}, \tilde{y}, \delta) &= \left( -\frac{2\delta r}{K} + \frac{\beta\delta y^*}{(\beta + x^*)^3} \right) \tilde{x}^2 - \frac{\beta\delta}{(\beta + x^*)^2} \tilde{x}\tilde{y} - \frac{\beta\delta y^*}{(\beta + x^*)^4} \tilde{x}^3 + \frac{\beta\delta}{(\beta + x^*)^3} \tilde{x}^2\tilde{y} + O(\|X\|^4), \\ F_2(\tilde{x}, \tilde{y}, \delta) &= -\frac{\alpha\beta\delta y^*}{(\beta + x^*)^3} \tilde{x}^2 + \frac{\alpha\beta\delta}{(\beta + x^*)^2} \tilde{x}\tilde{y} + \frac{\alpha\beta\delta y^*}{(\beta + x^*)^4} \tilde{x}^3 - \frac{\alpha\beta\delta}{(\beta + x^*)^3} \tilde{x}^2\tilde{y} + O(\|X\|^4), \end{aligned} \quad (15)$$

and  $X = (\tilde{x}, \tilde{y})^T$ . It follows that

$$\begin{aligned} B_1(x, y) &= \sum_{j,k=1}^2 \frac{\partial^2 F_1(\xi, \delta)}{\partial \xi_j \partial \xi_k} \Big|_{\xi=0} x_j y_k = \left( -\frac{2\delta r}{K} + \frac{2\beta\delta y^*}{(\beta + x^*)^3} \right) x_1 y_1 - \frac{\beta\delta}{(\beta + x^*)^2} (x_1 y_2 + x_2 y_1), \\ B_2(x, y) &= \sum_{j,k=1}^2 \frac{\partial^2 F_2(\xi, \delta)}{\partial \xi_j \partial \xi_k} \Big|_{\xi=0} x_j y_k = -\frac{2\alpha\beta\delta y^*}{(\beta + x^*)^3} x_1 y_1 + \frac{\alpha\beta\delta}{(\beta + x^*)^2} (x_1 y_2 + x_2 y_1), \\ C_1(x, y, u) &= \sum_{j,k,l=1}^2 \frac{\partial^3 F_1(\xi, \delta)}{\partial \xi_j \partial \xi_k \partial \xi_l} \Big|_{\xi=0} x_j y_k u_l = -\frac{6\beta\delta y^*}{(\beta + x^*)^4} x_1 y_1 u_1 + \frac{2\beta\delta}{(\beta + x^*)^3} (x_1 y_1 u_2 + x_1 y_2 u_1 + x_2 y_1 u_1), \\ C_2(x, y, u) &= \sum_{j,k,l=1}^2 \frac{\partial^3 F_2(\xi, \delta)}{\partial \xi_j \partial \xi_k \partial \xi_l} \Big|_{\xi=0} x_j y_k u_l = \frac{6\alpha\beta\delta y^*}{(\beta + x^*)^4} x_1 y_1 u_1 - \frac{2\alpha\beta\delta}{(\beta + x^*)^3} (x_1 y_1 u_2 + x_1 y_2 u_1 + x_2 y_1 u_1), \end{aligned}$$

and  $\delta = \delta_1$ .

Therefore,  $B(x, y) = \begin{pmatrix} B_1(x, y) \\ B_2(x, y) \end{pmatrix}$  and  $C(x, y, u) = \begin{pmatrix} C_1(x, y, u) \\ C_2(x, y, u) \end{pmatrix}$  are symmetric multilinear vector

functions of  $x, y, u \in \mathbb{R}^2$  and  $A(\delta) = J(x^*, y^*)$ .

We know that  $A$  has simple eigenvalue  $\lambda_1(\delta_1) = -1$ , and the corresponding eigenspace  $E^c$  is one-dimensional and spanned by an eigenvector  $q \in \mathbb{R}^2$  such that  $A(\delta_1)q = -q$ . Let  $p \in \mathbb{R}^2$  be the adjoint eigenvector, that is,  $A^T(\delta_1)p = -p$ . By direct calculation we obtain

$$q \sim (-2 - \delta_1 b_2, \delta_1 a_2)^T, \text{ and}$$

$$p \sim (-2 - \delta_1 b_2, -\delta_1 b_1)^T.$$

In order to normalize  $p$  with respect to  $q$ , we denote

$$p = \gamma_1 (-2 - \delta_1 b_2, -\delta_1 b_1)^T$$

where

$$\gamma_1 = \frac{1}{(-2 - \delta_1 b_2)^2 - \delta_1^2 a_2 b_1}.$$

It is easy to see  $\langle p, q \rangle = 1$ , where  $\langle \cdot; \cdot \rangle$  means the standard scalar product in  $\mathbb{R}^2$ :  $\langle p, q \rangle = p_1 q_1 + p_2 q_2$ .

Following the algorithms given in (Kuznetsov, 1998), the sign of the critical normal form coefficient  $c(\delta_1)$ , which determines the direction of the flip bifurcation, is given by the following formula:

$$c(\delta_1) = \frac{1}{6} \langle p, C(q, q, q) \rangle - \frac{1}{2} \langle p, B(q, (A - I)^{-1} B(q, q)) \rangle \tag{16}$$

From the above analysis and the theorem in (Kuznetsov, 1998; Guckenheimer and Holmes, 1983; Robinson, 1999; Wiggins, 2003), we have the following result.

**Theorem 1.** Suppose that  $(x^*, y^*)$  is the positive fixed point. If the conditions (12), (13) hold and  $c(\delta_1) \neq 0$ , then system (3) undergoes a flip bifurcation at the fixed point  $(x^*, y^*)$  when the parameter  $\delta$  varies in a small neighborhood of  $\delta_1$ . Moreover, if  $c(\delta_1) > 0$  (respectively,  $c(\delta_1) < 0$ ), then the period-2 orbits that bifurcate from  $(x^*, y^*)$  are stable (respectively, unstable).

In Section 4, we will give some values of the parameters such that  $c(\delta_1) \neq 0$ , thus the flip bifurcation occurs as  $\delta$  varies (see Figure 2).

We next discuss the existence of a Neimark-Sacker bifurcation by using the Neimark-Sacker theorem in (Kuznetsov, 1998; Guckenheimer and Holmes, 1983; Robinson, 1999; Wiggins, 2003).

It is clear that the eigenvalues  $\lambda_{1,2}$  given by (11) are complex for  $(trJ)^2 - 4 \det J < 0$ , which leads to  $\Delta < 0$ , i.e.,

$$(a_1 - b_2)^2 - 4a_2 b_1 < 0 \tag{17}$$

Let  $\delta = \delta_2 = -\frac{a_1 + b_2}{a_1 b_2 + a_2 b_1}$ ,

then we have  $\det J(\delta_2) = 1$ .

For  $\delta = \delta_2$ , the eigenvalues of the matrix associated with the linearization of the map (14) at  $(\tilde{x}, \tilde{y}) = (0,0)$  are conjugate with modulus 1, and they are written as

$$\begin{aligned} \lambda, \bar{\lambda} &= \frac{\text{tr}J(\delta_2)}{2} \pm \frac{i}{2} \sqrt{4\det J(\delta_2) - (\text{tr}J(\delta_2))^2} \\ &= 1 + \frac{\delta_2}{2}(a_1 + b_2) \pm \frac{i\delta_2}{2} \sqrt{4a_2b_1 - (a_1 - b_2)^2} \end{aligned} \quad (18)$$

$$\text{and } |\lambda(\delta_2)| = 1, \quad \left. \frac{d|\lambda(\delta)|}{d\delta} \right|_{\delta=\delta_2} = -\frac{1}{2}(a_1 + b_2) \neq 0.$$

In addition, if  $\text{tr}J(\delta_2) \neq 0, -1$ , which leads to

$$\delta_2(a_1 + b_2) \neq -2, -3,$$

then we have  $\lambda^k(\delta_2) \neq 1$  for  $k = 1, 2, 3, 4$ .

Let  $q \in \mathbb{C}^2$  be an eigenvector of  $A(\delta_2)$  corresponding to the eigenvalue  $\lambda(\delta_2)$  such that

$$A(\delta_2)q = \lambda(\delta_2)q, \quad A(\delta_2)\bar{q} = \bar{\lambda}(\delta_2)\bar{q}.$$

Also let  $p \in \mathbb{C}^2$  be an eigenvector of the transposed matrix  $A^T(\delta_2)$  corresponding to its eigenvalue, that is,  $\bar{\lambda}(\delta_2)$ ,

$$A^T(\delta_2)p = \bar{\lambda}(\delta_2)p, \quad A^T(\delta_2)\bar{p} = \lambda(\delta_2)\bar{p}.$$

By direct calculation we obtain

$$q \sim (1 + \delta_2 b_2 - \lambda, -\delta_2 a_2)^T,$$

$$p \sim (1 + \delta_2 b_2 - \bar{\lambda}, \delta_2 b_1)^T.$$

In order to normalize  $p$  with respect to  $q$ , we denote

$$p = \gamma_2 (1 + \delta_2 b_2 - \bar{\lambda}, \delta_2 b_1)^T$$

where

$$\gamma_2 = \frac{1}{(1 + \delta_2 b_2 - \bar{\lambda})^2 - \delta_2^2 a_2 b_1}.$$

It is easy to see  $\langle p, q \rangle = 1$ , where  $\langle \cdot, \cdot \rangle$  means the standard scalar product in  $\mathbb{C}^2$ :

$$\langle p, q \rangle = \bar{p}_1 q_1 + \bar{p}_2 q_2.$$

Any vector  $X \in \mathbb{R}^2$  can be represented for  $\delta$  near  $\delta_2$  as  $X = zq + \bar{z}\bar{q}$ , for some complex  $z$ . Indeed, the explicit formula to determine  $z$  is  $z = \langle p, X \rangle$ . Thus, system (14) can be transformed for sufficiently small  $|\delta|$  (near  $\delta_2$ ) into the following form:

$$z \mapsto \lambda(\delta)z + g(z, \bar{z}, \delta),$$

where  $\lambda(\delta)$  can be written as  $\lambda(\delta) = (1 + \varphi(\delta))e^{i\theta(\delta)}$  (where  $\varphi(\delta)$  is a smooth function with  $\varphi(\delta_2) = 0$ ) and  $g$  is a complex-valued smooth function of  $z, \bar{z}$ , and  $\delta$ , whose Taylor expression with respect to  $(z, \bar{z})$  contains quadratic and higher-order terms:

$$g(z, \bar{z}, \delta) = \sum_{k+l \geq 2} \frac{1}{k!l!} g_{kl}(\delta) z^k \bar{z}^l, \text{ with } g_{kl} \in \mathbb{C}, k, l = 0, 1, \dots$$

By symmetric multilinear vector functions, the Taylor coefficients  $g_{kl}$  can be expressed by the formulas

$$\begin{aligned} g_{20}(\delta_2) &= \langle p, B(q, q) \rangle, & g_{11}(\delta_2) &= \langle p, B(q, \bar{q}) \rangle, \\ g_{02}(\delta_2) &= \langle p, B(\bar{q}, \bar{q}) \rangle, & g_{21}(\delta_2) &= \langle p, C(q, q, \bar{q}) \rangle, \end{aligned}$$

and the coefficient  $a(\delta_2)$ , which determines the direction of the appearance of the invariant curve in a generic system exhibiting the Neimark-Sacker bifurcation, can be computed via

$$a(\delta_2) = \operatorname{Re} \left( \frac{e^{-i\theta(\delta_2)} g_{21}}{2} \right) - \operatorname{Re} \left( \frac{(1 - 2e^{i\theta(\delta_2)}) e^{-2i\theta(\delta_2)}}{2(1 - e^{i\theta(\delta_2)})} g_{20} g_{11} \right) - \frac{1}{2} |g_{11}|^2 - \frac{1}{4} |g_{02}|^2,$$

where  $e^{i\theta(\delta_2)} = \lambda(\delta_2)$ .

For the above argument and the theorem in (Kuznetsov, 1998; Guckenheimer and Holmes, 1983; Robinson, 1999; Wiggins, 2003), we have the following result.

**Theorem 2.** Suppose that  $(x^*, y^*)$  is the positive fixed point. If  $a(\delta_2) < 0$  (respectively,  $> 0$ ) the Neimark-Sacker bifurcation of system (3) at  $\delta = \delta_2$  is supercritical (respectively, subcritical) and there exists a unique closed invariant curve bifurcation from  $(x^*, y^*)$  for  $\delta = \delta_2$ , which is asymptotically stable (respectively, unstable).

In Section 4 we will choose some values of the parameters so as to show the process of a Neimark-Sacker bifurcation for system (3) in Figure 3 by numerical simulation.

#### 4 Numerical Simulations

In this section, by using numeral simulation, we give the bifurcation diagrams, phase portraits and Lyapunov exponents of the system (3) to confirm the previous analytic results and show some new interesting complex dynamical behaviors existing in the system (3). It is known that Maximum Lyapunov exponents quantify the

exponential divergence of initially close state-space trajectories and frequently employ to identify a chaotic behaviour. Based on the previous analysis, we choose the parameter  $\delta$  as a bifurcation parameter (varied parameter) and other model parameters are as fixed parameters, otherwise stated to study the flip bifurcation and Neimark-Sacker bifurcation for the unique positive fixed point. Without lose generality, the bifurcation parameters are considered in the following cases:

**Case (i):** varying  $\delta$  in range  $1.2 \leq \delta \leq 1.5$ , and fixing  $r = 2, K = 1.5, d = 0.25, \alpha = 0.75, \beta = 2.5$ .

**Case (ii):** varying  $\delta$  in range  $1.4 \leq \delta \leq 2.5$ , and fixing  $r = 2, K = 1, d = 0.2, \alpha = 0.85, \beta = 1.05$ .

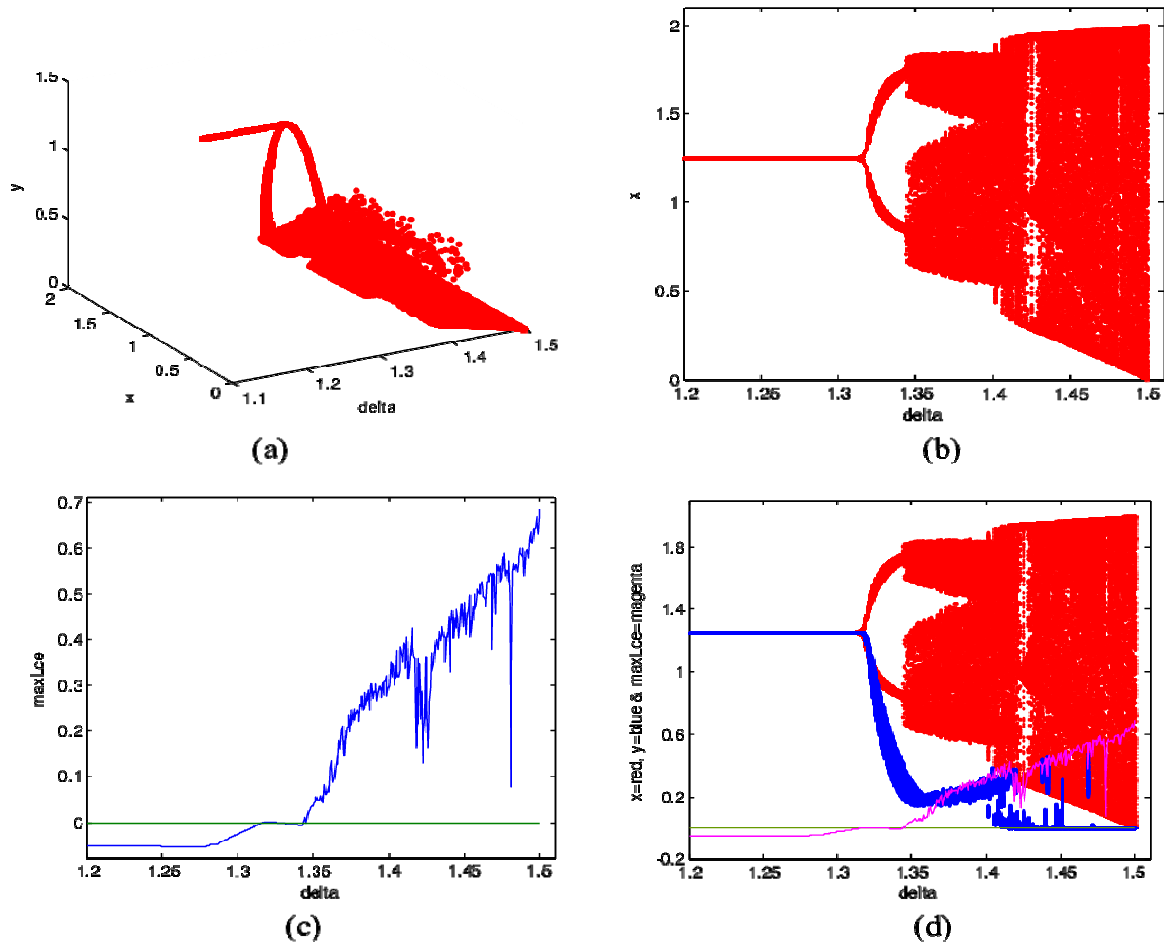


**Fig. 2** Bifurcation diagrams and maximum Lyapunov exponent for system (3) around  $E_2$ . (a) Flip bifurcation diagram of system (3) in  $(\delta - x - y)$  space, the initial value is  $(x_0, y_0) = (1.23, 1.23)$  (b) Flip bifurcation diagram in  $(\delta - x)$  plane (c) Maximum Lyapunov exponents corresponding to (b) and (d) Maximum Lyapunov exponents are superimposed on Flip bifurcation diagram.

For case (i). The bifurcation diagrams of system (3) in  $(\delta - x - y)$  space and in  $(\delta - x)$  pane are given in Fig. 2(a-b). After calculation for the fixed point  $E_2$  of map (3), the flip bifurcation emerges from the fixed point  $(1.25, 1.25)$  at  $\delta = \delta_1 = 1.31667$  and  $(r, K, d, \alpha, \beta) \in FB1_{E_2}$ . It shows the correctness of proposition 1. At  $\delta = \delta_1$ , we have  $c(\delta_1) = -0.632609$ , which determines the direction of the flip bifurcation and shows the correctness of Theorem1. From Fig. 2(b), we see that the fixed point  $E_2$  is stable for  $\delta < 1.31667$  and loses its stability at the flip bifurcation parameter value  $\delta = 1.31667$ , we also

observe that there is a cascade of period doubling bifurcations for  $\delta > 1.31667$ . The maximum Lyapunov exponents corresponding to Fig. 2(b) are computed and plotted in Fig. 2(c), confirming the existence of the chaotic regions and period orbits in the parametric space.

For case (ii). The bifurcation diagrams of system (3) in the  $(\delta - x - y)$  space, the  $(\delta - x)$  plane and the  $(\delta - y)$  plane are given in Fig. 3(a-b-c). After calculation for the fixed point  $E_2$  of map (3), the Neimark-Sacker bifurcation emerges from the fixed point  $(0.323077, 1.85893)$  at  $\delta = \delta_2 = 1.58217$  and  $(r, K, d, \alpha, \beta) \in NS_{E_2}$ . It shows the correctness of proposition 1. For  $\delta = \delta_2$ , we have

$$\lambda, \bar{\lambda} = 0.740839 \pm 0.671682 i, \quad |\lambda| = 1, |\bar{\lambda}| = 1, \quad \left. \frac{d|\lambda(\delta)|}{d\delta} \right|_{\delta=\delta_2} = 0.163801 > 0,$$

$$\delta_2(a_1 + b_2) = -0.518321 \neq -2, -3, \quad g_{20} = 2.14989 - 0.275425 i, \quad g_{11} = 0.571595 - 1.26846 i,$$

$$g_{02} = 0.00135796 + 2.39002 i, \quad g_{21} = -2.09682 - 0.425716 i, \quad \text{and } a(\delta_2) = -3.31917. \text{ Therefore, the}$$

Neimark-Sacker bifurcation is supercritical and it shows the correctness of Theorem 2.

From Fig. 3(b-c), we observe that the fixed point  $E_2$  of map (3) is stable for  $\delta < 1.58217$  and loses its stability at  $\delta = 1.58217$  and an invariant circle appears when the parameter  $\delta$  exceeds 1.58217, we also observe that there are period-doubling phenomenons. The maximum Lyapunov exponents corresponding to Fig. 3(b-c) are computed and plotted in Fig. 3(d), confirming the existence of the chaotic regions and period orbits in the parametric space. From Fig. 3(d), we observe that some Lyapunov exponents are bigger than 0, some are smaller than 0, so there exist stable fixed points or stable period windows in the chaotic region. In general the positive Lyapunov exponent is considered to be one of the characteristics implying the existence of chaos. The bifurcation diagrams for  $x$  and  $y$  together with maximum Lyapunov exponents is presented in Fig. 3(e). Fig. 3(f) is the local amplification corresponding to Fig. 3(b) for  $\delta \in [2.005, 2.2206]$ .

The phase portraits which are associated with Fig. 3(a) are disposed in Fig. 4, which clearly depicts the process of how a smooth invariant circle bifurcates from the stable fixed point  $(0.323077, 1.85893)$ . When  $\delta$  exceeds 1.58217, there appears a circular curve enclosing the fixed point  $E_2$ , and its radius becomes larger with respect to the growth of  $\delta$ . When  $\delta$  increases at certain values, for example, at  $\delta = 2.04$ , the circle disappears and a period-7 orbits appears, and some cascades of period doubling bifurcations lead to chaos. From Fig. 4, we observe that as  $\delta$  increases there are period-7, 20-orbits, quasi-periodic orbits and attracting chaotic sets. See that for  $\delta = 2.3357, 2.45$  &  $2.5$ , where the system is chaotic, the value of maximal Lyapunov exponent is positive that confirm the existence of the chaotic sets.

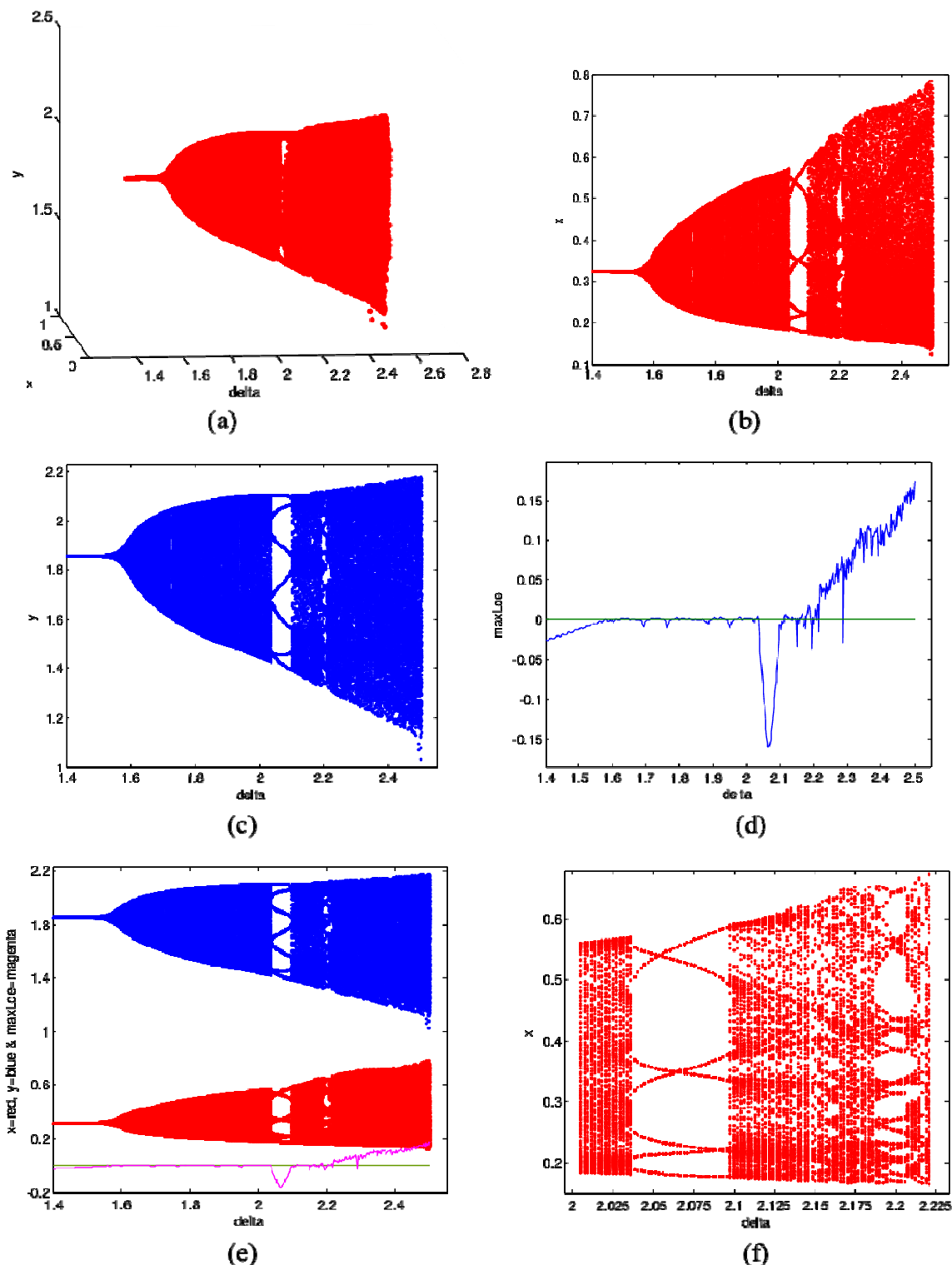


**Fig. 3** Bifurcation diagrams and maximum Lyapunov exponent for system (3) around  $E_2$ . (a) Neimark-Sacker bifurcation diagram of system (3) in  $(\delta - x - y)$  space (b-c) Neimark-Sacker bifurcation diagrams in  $(\delta - x)$  and  $(\delta - y)$  planes (d) Maximum Lyapunov exponents corresponding to (b-c) (e) Maximum Lyapunov exponents are superimposed on bifurcation diagrams (f) Local amplification corresponding to (b) for  $\delta \in [2.005, 2.2206]$ . The initial value is  $(x_0, y_0) = (0.3, 1.8)$ .

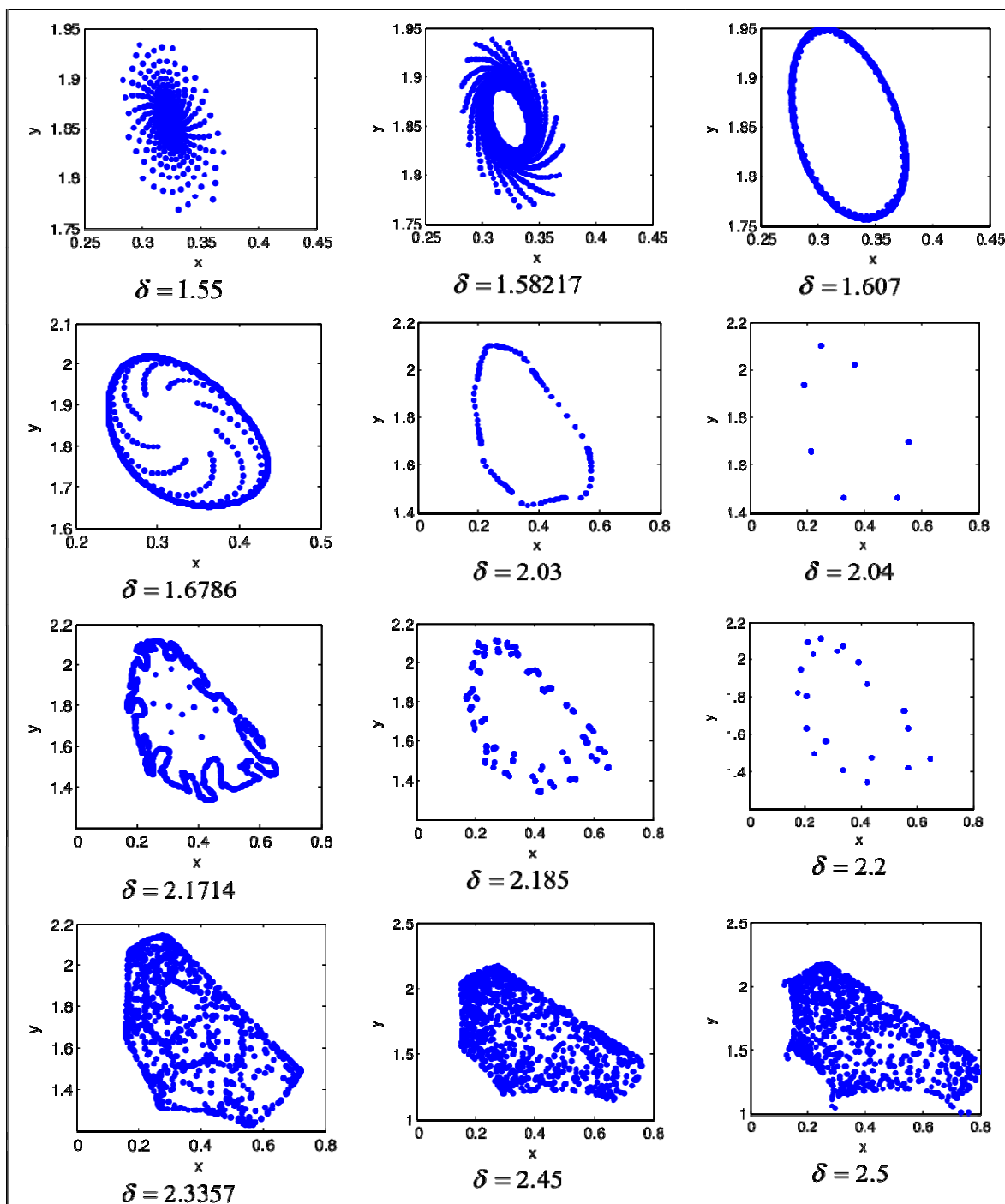
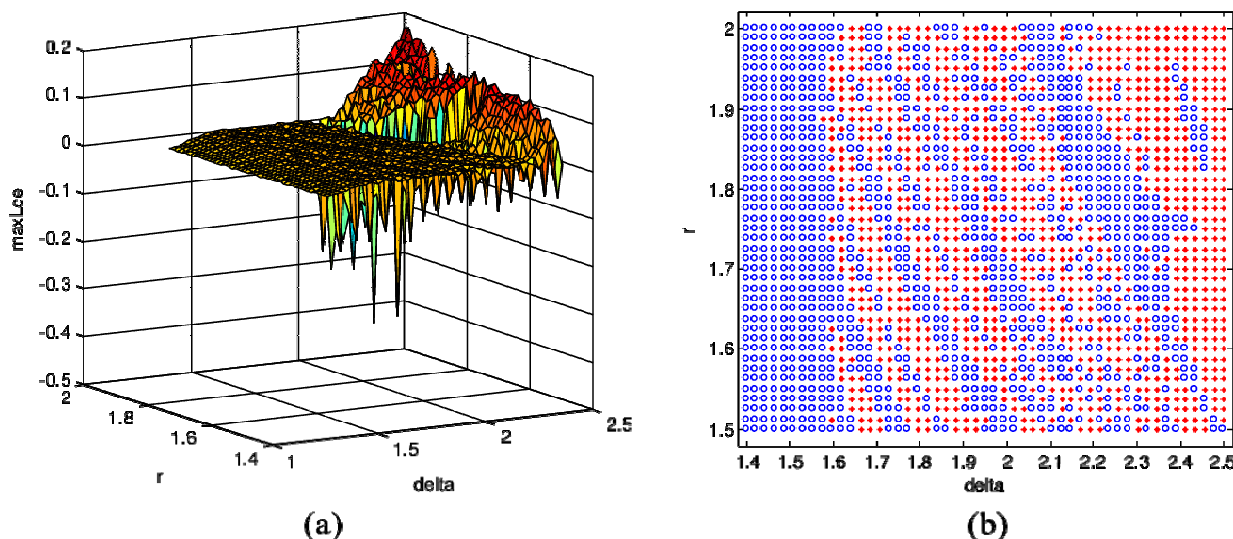


Fig. 4 Phase portraits for various values of  $\delta$  corresponding to Fig. 3(a).

In order to observe the complex dynamics, we can vary one more parameters of system (3). Since the values of Lyapunov exponents quantify the chaotic behavior of discrete system or at least sensitive dependence on initial conditions, so we compute maximum Lyapunov exponents of system (3) and study the dependence of these Lyapunov exponents on two real parameters  $\delta$  and  $r$ . The maximum Lyapunov exponents of system (3) for parameters  $\delta \in [1.4, 2.5]$  and  $r \in [1.5, 2.0]$  and fixing other parameters as in case (ii) is given in Fig. 5(a). In Fig. 5(b) is plotted the sign of the maximal Lyapunov exponent of map (3). Blue color represents negative Lyapunov exponent and red color represents positive Lyapunov exponent. Here it is easy

to see for which choice of parameters the system (3) is showing chaotic motion, and for which one is the system (3) exhibiting periodic or quasi periodic movement. E.g., the chaotic situation is on Fig. 4 for values of parameters  $\delta = 2.5$  &  $r = 2$  and the non-chaotic situation is for values of parameters  $\delta = 2.2$  &  $r = 2$  which are consistent with signs in Fig. 5(b). Fig. 6 is plotted sign of the maximum Lyapunov exponents of system (3) covering  $\delta \in [1.4, 1.85]$ ,  $\beta \in [0.9, 1.05]$  and  $\delta \in [1.4, 2.5]$ ,  $\beta \in [1.05, 1.3]$ , respectively and fixing other parameters as in case (ii). It shows that the dynamics of the system (3) is chaotic for small values of the parameter  $\beta$ .



**Fig. 5** Sign of maximum Lyapunov exponent for system (3) around  $E_2$ . (a) Maximum Lyapunov exponents of system (3) covering  $\delta \in [1.4, 2.5]$ ,  $r \in [1.5, 2.0]$ , and  $K = 1, d = 0.2, \alpha = 0.85, \beta = 1.05$  (b) Sign of Maximum Lyapunov exponents corresponding to (a) (red '+' = positive, blue 'o' = negative). The initial value is  $(x_0, y_0) = (0.3, 1.8)$ .

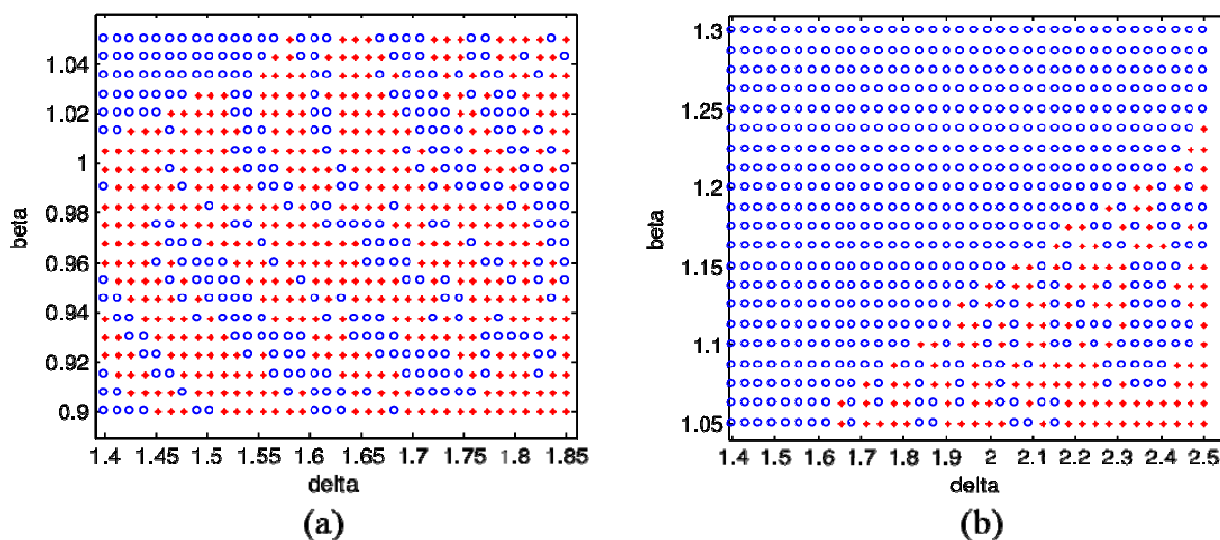


**Fig. 6** Sign of maximum Lyapunov exponent for system (3) around  $E_2$ . (a) Sign of Maximum Lyapunov exponents of system (3) covering  $\delta \in [1.4, 1.85]$ ,  $\beta \in [0.9, 1.05]$  and  $r = 2, K = 1, d = 0.2, \alpha = 0.85$  (b) Sign of Maximum Lyapunov exponents covering  $\delta \in [1.4, 2.5]$ ,  $\beta \in [1.05, 1.3]$  (red '+' = positive, blue 'o' = negative).

## 5 Discussion

In this paper, we investigated the behaviors of the discrete-time predator-prey system (3) involving group defense with Holling type II functional response and showed that it has a complex dynamics in the closed first quadrant  $R_+^2$ . We showed that the unique positive fixed point of (3) can undergo a flip bifurcation and a Neimark-Sacker bifurcation under certain parametric conditions. Moreover, as the parameters varying, the system (3) exhibits the variety of dynamical behaviors, including period-7, 20-orbits, invariant cycle, cascade of period-doubling, quasi-periodic orbits and the chaotic sets, which imply that the predators and prey can coexist in the stable period-n orbits and invariant cycle. Finally, simulation works showed that in certain regions of the parameter space, the model (3) had a great sensitivity to the choice of initial conditions and parameter values. These results reveal far richer dynamics of the discrete model compared to the continuous model.

## References

- Agiza HN, Elabbasy EM, EL-Metwally H, et al. 2009. Chaotic dynamics of a discrete prey-predator model with Holling type II. *Nonlinear Analysis: Real World Applications*, 10: 116-129
- Brauer F, Castillo-Chavez C. 2001. *Mathematical models in population biology and epidemiology*. Springer-Verlag, New York, USA
- Danca M, Codreanu S, Bako B. 1997. Detailed analysis of a nonlinear prey-predator model. *Journal of Biological Physics*, 23: 11-20
- Elsadany AA, EL-Metwally HA, Elabbasy EM, Agiza HN. 2012. Chaos and bifurcation of a nonlinear discrete prey-predator system. *Computational Ecology and Software*, 2(3): 169-180
- Elaydi SN. 1996. *An Introduction to Difference Equations*. Springer-Verlag Publishers
- Freedman HI, Wolkowicz GS. K. 1986. Predator-prey systems with group defense: The paradox of enrichment revisited, *Bull. Math. Biol.* 48: 493-508
- Ghaziani R. K. 2014. Dynamics and bifurcations of a Lotka-Volterra population model. *Iranian Journal of Science & Technology*, 38A3: 265-279
- Guckenheimer J, Holmes P. 1983. *Nonlinear Oscillations, Dynamical Systems, and Bifurcations of Vector Fields*. Springer, New York, USA
- Hasan KA, Hama, MF. 2012. Complex Dynamics Behaviors of a Discrete Prey-Predator Model with Beddington-DeAngelis Functional Response. *Int. J. Contemp. Math. Sciences*, 7(45): 2179-2195
- Hastings A, Powell T. 1991. Chaos in three-species food chain. *Ecology*, 72: 896-903
- He ZM, Lai X. 2011. Bifurcations and chaotic behavior of a discrete-time predator-prey system. *Nonlinear Analysis: Real World Applications*, 12: 403-417
- He ZM, Li Bo. 2014. Complex dynamic behavior of a discrete-time predator-prey system of Holling-III type. *Advances in Difference Equations*, 180
- Hu ZY, Teng Z, Zhang L. 2011. Stability and bifurcation analysis of a discrete predator-prey model with nonmonotonic functional response. *Nonlinear Analysis*, 12: 2356-2377
- Jing ZJ, Yang J. 2006. Bifurcation and chaos discrete-time predator-prey system. *Chaos, Solutions and Fractals*, 27: 259-277
- Holling CS. 1965. The functional response of predator to prey density and its role in mimicry and population regulation. *Memoirs of the Entomological Society of Canada*, 45: 1-60
- Klebanoff A, Hastings A. 1994. Chaos in three species food-chain. *Journal of Mathematical Biology*, 32: 427-

245

- Kuznetsov, YK. 1998. Elements of Applied Bifurcation Theory, 3rd edn. Springer, New York, USA
- Li TY, Yorke JA. 1975. Period three implies chaos. Amer Math Monthly; 82:985-992
- Liu X, Xiao DM. 2007. Complex dynamic behaviors of a discrete-time predator-prey system. Chaos, Solutions and Fractals, 32: 80-94
- Lotka AJ. 1925. Elements of mathematical biology, Williams and Wilkins, Baltimore, USA
- Murray JD. 1998. Mathematical Biology. Springer-Verlag, Berlin, Germany
- Rana SM. 2015. Bifurcation and complex dynamics of a discrete-time predator-prey system. Computational Ecology and Software. 5(2): 187-200
- Robinson C. 1999. Dynamical Systems, Stability, Symbolic Dynamics and Chaos (2nd edn) . CRC Press, Boca Raton, USA
- Rosenzweig ML, MacArthur RH. 1963. Graphical representation and stability conditions of predator-prey interactions. American Naturalist.97:209-23
- Volterra V. 1926. Variazioni e fluttuazioni del numero d'individui in specie animali conviventi, Mem. R. Accad. Naz. Dei Lincei, Ser. VI, vol. 2
- Wang C, Li X. 2014. Stability and Neimark-Sacker bifurcation of a semi-discrete population model. Journal of Applied Analysis and Computation. V4 (4): 419-435
- Wiggins S. 2003. Introduction to Applied Nonlinear Dynamical Systems and Chaos (2nd edn) . Springer, New York, USA
- Zhu H, Campbell SA, Wolkowicz G. 2002. Bifurcation analysis of a predator-prey system with nonmonotonic functional response. SIAM Journal on Applied Mathematics, 63: 636-682